AFRL-SN-RS-TR-2006-129
Final Technical Report
April 2006

A COMPREHENSIVE APPROACH TO ADAPTIVE PROCESSING BOTH ON TRANSMIT AND RECEIVE INCLUDING PRESENCE OF WAVEFORM DIVERSITY

Syracuse University

APPROVED FOR PUBLIC RELEASE; DISTRIBUTION UNLIMITED.

AIR FORCE RESEARCH LABORATORY
SENSORS DIRECTORATE
ROME RESEARCH SITE
ROME, NEW YORK

STINFO FINAL REPORT

This report has been reviewed by the Air Force Research Laboratory, Information Directorate, Public Affairs Office (IFOIPA) and is releasable to the National Technical Information Service (NTIS). At NTIS it will be releasable to the general public, including foreign nations.

AFRL-SN-RS-TR-2006-129 has been reviewed and is approved for publication

APPROVED: /s/

PETER A. ZULCH
Project Engineer

FOR THE DIRECTOR: /s/

RICHARD G. SHAUGHNESSY
Chief, Rome Operations Office
Sensors Directorate

REPORT DOCUMENTATION PAGE

Form Approved
OMB No. 074-0188

1. AGENCY USE ONLY (Leave blank)

2. REPORT DATE
APRIL 2006

3. REPORT TYPE AND DATES COVERED
Final Aug 01 – Aug 05

4. TITLE AND SUBTITLE
A Comprehensive Approach to Adaptive Processing Both on Transmit and Receive Including Presence of Waveform Diversity

5. FUNDING NUMBERS
C - F30602-01-1-0545
PE - 62204F
PR - 762R
TA - SN
WU - P8

6. AUTHOR(S)
Tapan K. Sarkar

7. PERFORMING ORGANIZATION NAME(S) AND ADDRESS(ES)
Syracuse University
Department of Electrical Engineering and Computer Science
Syracuse, New York 13244-1240

8. PERFORMING ORGANIZATION REPORT NUMBER
N/A

9. SPONSORING / MONITORING AGENCY NAME(S) AND ADDRESS(ES)
Air Force Research Laboratory/SNRT
26 Electronic Parkway
Rome New York 13441-4514

10. SPONSORING / MONITORING AGENCY REPORT NUMBER
AFRL-SN-RS-TR-2006-129

11. SUPPLEMENTARY NOTES

AFRL Project Engineer: Peter A. Zulch/AFRL/SNRT/(315) 330-7861 Peter.Zulch@rl.af.mil

12a. DISTRIBUTION / AVAILABILITY STATEMENT

APPROVED FOR PUBLIC RELEASE; DISTRIBUTION UNLIMITED.

12b. DISTRIBUTION CODE

13. ABSTRACT *(Maximum 200 Words)*

In this final report, the quality of the adaptive processing is investigated as a function of random position errors in the locations of the sensors. Use of waveform diversity and a comprehensive approach to adaptive processing may not be useful if the sensors deviate from their true positions, due to environmental effects or due to mechanical errors in their positioning. Here, we provide an upper bound for the spatial variations in the locations of the sensors, implying that if the errors are within this bound then acceptable performance can be expected. The equivalent isotropically radiated power (EIRP) degradation due to random position errors for Space-Time Adaptive Processing (STAP) is presented based on the relationship between the EIRP degradation and the standard deviation or the uniform bound of the probability distribution of location of the antenna elements. We simulate a direct data domain least squares (D^3LS) approach for STAP under two different conditions. In the first case, the antenna elements at every time instance are assumed to have different spatial positions from the previous time instance. For the other case, the antennas are assumed to be randomly located, but are assumed to be fixed in a coherent processing interval (CPI). It is demonstrated that whether the locations of the antenna are fixed or they vary within a CPI with identical random errors, the output signal to interference and noise ratio (SINR) are almost the same. When the antenna elements are moved randomly, the output SINR is less than the unperturbed case. We can develop a bound on the EIRP degradation due to the D^3LS approach to STAP based on the random position errors.

14. SUBJECT TERMS
Space Time Adaptive Processing, Random Position Errors, Waveform diversity

15. NUMBER OF PAGES
24

16. PRICE CODE

17. SECURITY CLASSIFICATION OF REPORT	18. SECURITY CLASSIFICATION OF THIS PAGE	19. SECURITY CLASSIFICATION OF ABSTRACT	20. LIMITATION OF ABSTRACT
UNCLASSIFIED	UNCLASSIFIED	UNCLASSIFIED	UL

Table of Contents

List of Figures

List of Tables

1. Summary of Research Carried out in this Contract

In this research, the goal was to develop techniques on how to enhance the received signals in a near field multi-input multi-output (MIMO) environment where beam forming is not possible. This is done through the use of adaptivity on transmit. This technique is based on the principle of reciprocity, is independent of the material medium in which it is transmitting, and incorporates near-field environments and multipath. The objective here is to select a set of weights adapted to each receiver to be applied to each transmitting antenna, which is a function of the user location, so that the transmitted signal at the carrier frequency may be directed to a particular receiver location while simultaneously minimizing the received signal strengths at other receiver locations.

Next the principles of polarization was utilized. The polarization adaptivity on transmit can be used to enhance the received signals directed to a pre-selected receiver in a near-field multi-input multi-output (MIMO) environment. The objective here is to select a set of weights on the transmitting antennas adapted to each receiver based on the principles of reciprocity. Using the polarization properties, when the number of receiving antennas is greater than the number of transmitting antennas, the transmitted signal may be directed more to a particular receiver location while simultaneously minimizing the reception signal strength at other receivers. Wideband performance of this system has also been studied.

In addition, the effect of errors on the spatial location of antennas and how they impact the performance in adaptive processing for antenna arrays including its effect on STAP had also been studied. This final report deals with this topic.

2. Introduction

The direct data domain least squares (D^3LS) approaches are based on the work of Sarkar and Sangruji [1]. Then Sarkar et al [3, 4] presented two more variations to this approach, the Backward processor and the Forward-Backward processor. These algorithms were then extended to the space-time domain, where Park [5] described a generalized eigenvalue based processor and Sarkar et. al. [6] implemented the D^3LS processors.

The direct data domain least squares space-time adaptive processing (D^3LS STAP) algorithm has been used for suppressing highly dynamic clutter and interference [6-8]. This enables the system to detect potentially weak target returns. In this analysis, we assume that the system consists of a linear array of N equally spaced antenna elements. We assume that the system processes a number of pulses (M) within a coherent processing interval (CPI). Each pulse repetition interval (PRI) consists of the transmission of a pulsed waveform of finite bandwidth and the reception of the reflected energy by the radar aperture and receivers, with a bandwidth matched to that of the radar pulse. Data can be arranged into a three-dimensional matrix commonly referred to as a data cube [7]. We assume that the signals entering the array are narrowband, with a planar phase front, and consist of a signal-of-interest (SOI) along with interference plus noise. The noise (thermal noise) originates in the receiver and is understood to be independent across elements and pulses. The interference is external to the receiver and consists of clutter, jammers, and signal multipath, which may be coherent or incoherent. For a uniformly spaced linear array (ULA), the complex envelope of the received SOI with unity amplitude, for the m^{th} pulse and n^{th} antenna element, can be described by

$$S_{m,n} = \exp[\,j2\pi\{\frac{(n-1)\mathrm{d}}{\lambda}\cos(\phi_s) + \frac{(m-1)\mathrm{f_d}}{\mathrm{f_r}}\}],\ \text{for m = 1, 2, …, M; n = 1, 2, …, N} \qquad (1)$$

where d is the inter-element spacing between the antenna elements, λ is the wavelength, f_r is the pulse repetition frequency, ϕ_s is the angle of arrival and f_d is the Doppler frequency of the SOI. For the n^{th} antenna element and m^{th} pulse, the complex envelope of the received signal is given by the scalar quantity

$$X_{m,n} = \alpha_s \cdot S_{m,n} + \text{Interference} + \text{Noise} \qquad (2)$$

where α_s is the complex amplitude of the SOI entering the array. Between the scalars $X_{m,n}$ and $X_{m,n+1}$, there is a phase difference only for the SOI, which is given by [6, 8]

$$Z_1 = \exp[\,j2\pi\frac{\mathrm{d}}{\lambda}\cos(\phi_s)] \qquad (3)$$

Also, there is a phase difference for the SOI in the scalars $X_{m+1,n}$ and $X_{m,n}$,, due to the Doppler of the SOI, which is given by [6, 8]

$$Z_2 = \exp(j2\pi \frac{f_d}{f_r}) \tag{4}$$

For the two-dimensional case these differencing are performed with elements offset in space due to the subscript m, and in time due to the subscript n, and jointly in space and time due to the subscripts m+1, n+1 [6, 8]. The three types of difference equations are then given by

$$X_{m,n} - Z_1^{-1} \cdot X_{m,n+1} \tag{5}$$

$$X_{m,n} - Z_2^{-1} \cdot X_{m+1,n} \tag{6}$$

$$X_{m,n} - Z_1^{-1} \cdot Z_2^{-1} \cdot X_{m+1,n+1} \tag{7}$$

Now, we can form the cancellation rows in matrix [F], whose elements are generated using equations (5)-(7) [6, 8], which will deal with only the undesired signals, as the SOI has been cancelled out of equations (5)-(7). And the elements of the first row of matrix [F] is implemented by fixing the gain of the array along the direction of the SOI in both space and time as

$$[1, Z_1, Z_1^2, \cdots, Z_1^{N_a-1}, Z_2, Z_1 Z_2, Z_1^2 Z_2, \cdots Z_1^{N_a-1} Z_2, Z_2^2, Z_1 Z_2^2, \cdots, Z_1^{N_a-1} Z_2^{N_t-1}] \tag{8}$$

where N_a is the spatial dimension and N_t is the temporal dimension of the window. N_a and N_t must satisfy the following equations

$$N_a \le \frac{N+1}{2} \tag{9}$$

$$N_t \le \frac{M+1}{2} \tag{10}$$

The resulting matrix equation is then given by

$$[F][W] = [Y] = \begin{bmatrix} C & 0 & \dots & 0 \end{bmatrix}^T . \tag{11}$$

where [W] is the two-dimensional STAP weight vectors and C is the scalar gain of the array along the SOI in space and time.

The second process is to use Backward processor, which can be implemented by conjugating the element-pulse data and processing this data in reverse. We also use Forward-Backward process that is formed by combining the Forward and Backward solution procedure [3, 4].

When a D[3]LS STAP is used, we assume that each antenna element is designated to be placed at a specific location [8]. In the real environment, however, it is possible for the location of the antenna elements to fluctuate due to an installation error or environmental effects. Research on random perturbations in the excitation coefficients of the antenna arrays has been the subject of several papers [9, 10]. These papers consider random perturbations of the amplitude and phase of the amplifiers. As a follow-on to the paper by Zaghloul [9] on the deterioration of the equivalent isotropically radiated power (EIRP) due to random perturbations in the excitation coefficients of the antenna array, Hwang and Sarkar [12] present a paper for allowable tolerances in the position of antenna elements for acceptable performance. In this paper we identify how random position errors can affect a D[3]LS approach when applied to STAP. Our goal is to find how the system will perform when the antenna elements are randomly moved.

In Section II, we discuss EIRP degradation of the array antennas due to random position errors in terms of the normalized EIRP degradation. In Section III, to explore the utility of the EIRP degradation, a probabilistic analysis of a simple phased array antenna is studied. In Section IV, the D[3]LS approaches for STAP are simulated using the relationship between the EIRP degradation and position errors due to random locations of the elements in an array.

3. EIRP Degradation of Array Antennas Due to Random Position Errors

Consider an antenna array consisting of *N* antenna elements fed by *N* separate amplifiers. Except for a scaling factor, the far field $E(\theta,\phi)$ is given by

$$E(\theta,\phi) = \sum_{i=1}^{N} a_i \, e^{j(u x_i + v y_i + w z_i)} \, E_{el}(\theta,\phi) \tag{12}$$

where

$a_i = |a_i| e^{j\psi_i}$ complex excitation coefficient for the i^{th} antenna element

x_i = the random perturbation of the x-coordinate of the i^{th} antenna element

y_i = the random perturbation of the y-coordinates of the i^{th} antenna element

z_i = the random perturbation of the z-coordinates of the i^{th} antenna element

$u = k\sin\theta\cos\phi$, $v = k\sin\theta\sin\phi$, $w = k\cos\theta$, $k = 2\pi/\lambda$

$E_{el}(\theta,\phi)$ = the antenna element pattern along the direction (θ,ϕ).

The probability density functions of the random perturbations x_i, y_i, and z_i may be uniform or have Gaussian distributions. For uniform distributions, the probability density of x_i, y_i, and z_i are given by

$$p(x_i) = \frac{1}{2\Delta_x}, \quad \bar{x}_i - \Delta_x < x_i < \bar{x}_i + \Delta_x \qquad (13)$$
$$= 0, \qquad \text{otherwise}$$

$$p(y_i) = \frac{1}{2\Delta_y}, \quad \bar{y}_i - \Delta_y < y_i < \bar{y}_i + \Delta_x \qquad (14)$$
$$= 0, \qquad \text{otherwise}$$

$$p(z_i) = \frac{1}{2\Delta_z}, \quad \bar{z}_i - \Delta_z < z_i < \bar{z}_i + \Delta_x \qquad (15)$$
$$= 0, \qquad \text{otherwise}$$

For Gaussian distributions, the probability density functions for x_i, y_i, and z_i are given by

$$p(x_i) = \frac{1}{\sqrt{2\pi}\sigma_x} e^{-(x_i - \bar{x}_i)^2/2\sigma_x^2} \qquad (16)$$

$$p(y_i) = \frac{1}{\sqrt{2\pi}\sigma_y} e^{-(y_i - \bar{y}_i)^2/2\sigma_y^2} \qquad (17)$$

$$p(z_i) = \frac{1}{\sqrt{2\pi}\sigma_z} e^{-(z_i - \bar{z}_i)^2/2\sigma_z^2} \qquad (18)$$

where $\bar{x}_i, \bar{y}_i$ and $\bar{z}_i$ are the mean values of the x_i, y_i, and z_i-positions respectively, and σ_x^2, σ_y^2 and σ_z^2 are the variance of the x, y and z-coordinates respectively.

According to Zaghloul [9], EIRP along the direction (θ,ϕ) is proportional to the power radiated in the same direction. Therefore EIRP, is given by

$$P = \sum_{i=1}^{N} |G_i|^2 + \sum_{i=1}^{N} \sum_{\substack{j=1 \\ i \neq j}}^{N} e^{j[u(x_i - x_j) + v(y_i - y_j) + w(z_i - z_j)]} G_i G_j^* \qquad (19)$$

in which * denotes the complex conjugate, and

$$G_i = a_i \cdot E_{el}(\theta,\phi). \tag{20}$$

The probability distribution of the EIRP will be Gaussian with the mean value of P denoted by $\overline{P}$ and a standard deviation of $\sigma(P)$ from the central limit theory [11]. The probability distribution of the EIRP is within the confidence interval $\left[\overline{P} - n\sigma(P)]/P_0,\ [\overline{P} + n\sigma(P)]/P_0\right]$. Left side of the confidence interval in the probability distribution of the EIRP, $[\overline{P} - n\sigma(P)]/P_0$, represents the worst case for all possible cases. Normalizing $\overline{P}$ and $\sigma(P)$ with respect to the unperturbed power P_0 presents the degradation in the EIRP of the array. This quantity, $[\overline{P} - n\sigma(P)]/P_0$, is the normalized EIRP degradation. Along the same line of the amplitude and phase perturbation in reference [9], we choose $n = 3$ so that the worst-case degradation of the EIRP is within 99.7 percent of all possible cases for the given random position distributions.

The expected value $\overline{P}$ and the standard deviation $\sigma(P)$ of P can be expressed in separable terms containing the statistical parameters for x_i, y_i and z_i. Each amplifier is located at each x, y, and z-position and is considered to be independent. They have the same distribution. An expression for the influence of random locations of the antenna elements can be calculated by integrating the product of the probability distribution and the power P. The expected value $\overline{P}$ is obtained as

$$\overline{P} = \sum_{i=1}^{N} \left|G_i\right|^2 + \overline{H}_x \overline{H}_y \overline{H}_z \sum_{i=1}^{N} \sum_{j=1}^{N} e^{j[u(\overline{x}_i - \overline{x}_j) + v(\overline{y}_i - \overline{y}_j) + w(\overline{z}_i - \overline{z}_j)]} G_i G_j^* \tag{21}$$

where $\overline{H}_x$ is the x-position variation dependent factor, $\overline{H}_y$ is the y-position variation dependent factor and $\overline{H}_z$ is the z-position variation dependent factor. These expressions are given in Table 1.

Table 1: x, y and z-position Factors in the Expected Value Expression.

Factor	Uniform Distribution	Gaussian Distribution
$\overline{H}_x$	$(\sin u\Delta_x / u\Delta_x)^2$	$e^{-u^2\sigma_x^2}$
$\overline{H}_y$	$(\sin v\Delta_y / v\Delta y)^2$	$e^{-v^2\sigma_y^2}$
$\overline{H}_z$	$(\sin w\Delta_z / w\Delta_z)^2$	$e^{-w^2\sigma_z^2}$

The next step in calculating the standard deviation $\sigma(P)$ indicates the extent of the array EIRP degradation. The standard deviation is given by

$$\sigma(P) = \sqrt{\mathrm{var}(P)} \tag{22}$$

and the variance is defined as

$$\mathrm{var}(P) = \mathrm{E}[P^2] - \overline{P}^2 \tag{23}$$

in which $\mathrm{E}[\cdot]$ denotes the expectation value. We obtain $\mathrm{E}[P^2]$ as

$$\begin{aligned}
\mathrm{E}[P^2] = {} & \sum_{i=1}^{N} \left|G_i\right|^4 + 2\times \sum_{\substack{i=1 \\ i\neq j}}^{N}\sum_{j=1}^{N} \left|G_i\right|^2 \left|G_j\right|^2 + 4\times H_{1,x}H_{1,y}H_{1,z} \sum_{\substack{i=1 \\ i\neq j}}^{N}\sum_{j=1}^{N} e^{j[u(\overline{x}_i-\overline{x}_j)+v(\overline{y}_i-\overline{y}_j)+w(\overline{z}_i-\overline{z}_j)]} \left|G_i\right|^2 G_i G_j^* \\
& + 4\times H_{1,x}H_{1,y}H_{1,z} \sum_{k=1}^{N}\sum_{\substack{i=1 \\ k\neq i\neq j}}^{N}\sum_{j=1}^{N} e^{j[u(\overline{x}_i-\overline{x}_j)+v(\overline{y}_i-\overline{y}_j)+w(\overline{z}_i-\overline{z}_j)]} \left|G_k\right|^2 G_i G_j^* \\
& + H_{2,x}H_{2,y}H_{2,z} \sum_{\substack{i=1 \\ i\neq j}}^{N}\sum_{j=1}^{N} e^{j2[u(\overline{x}_i-\overline{x}_j)+v(\overline{y}_i-\overline{y}_j)+w(\overline{z}_i-\overline{z}_j)]} G_i^2 G_j^{*2} \\
& + H_{3,x}H_{3,y}H_{3,z} \sum_{k=1}^{N}\sum_{\substack{i=1 \\ k\neq i\neq j}}^{N}\sum_{j=1}^{N} [e^{j[u(\overline{x}_k+\overline{x}_i-2\overline{x}_j)+v(\overline{y}_k+\overline{y}_i-2\overline{y}_j)+w(\overline{z}_k+\overline{z}_i-2\overline{z}_j)]} G_k G_i G_j^{*2} \\
& \qquad + e^{j[u(-\overline{x}_k+2\overline{x}_i-\overline{x}_j)+v(-\overline{y}_k+2\overline{y}_i-\overline{y}_j)+w(-\overline{z}_k+2\overline{z}_i-\overline{z}_j)]} G_k G_i^2 G_j^*] \\
& + H_{4,x}H_{4,y}H_{4,z} \sum_{k=1}^{N}\sum_{\substack{l=1 \\ k\neq l\neq i\neq j}}^{N}\sum_{i=1}^{N}\sum_{j=1}^{N} e^{j[u(\overline{x}_k-\overline{x}_l+\overline{x}_i-\overline{x}_j)+v(\overline{y}_k-\overline{y}_l+\overline{y}_i-\overline{y}_j)+w(\overline{z}_k-\overline{z}_l+\overline{z}_i-\overline{z}_j)]} G_k G_l^* G_i G_j^*
\end{aligned} \tag{24}$$

where the factors $H_{*,x}$, $H_{*,y}$, and $H_{*,z}$ result from estimating constituents of the second moment of the power P, and are given in Table 2 for the Uniform and Gaussian distributions.

Table 2: x, y and z-position Factors in the Variance Expression.

Factor	Uniform Distribution	Gaussian Distribution
$H_{1,x}$	$\left(\frac{\sin u\Delta_x}{u\Delta_x}\right)^2$	$e^{-u^2\sigma_x^2}$
$H_{1,y}$	$\left(\frac{\sin v\Delta_y}{v\Delta_y}\right)^2$	$e^{-v^2\sigma_y^2}$
$H_{1,z}$	$\left(\frac{\sin w\Delta_z}{w\Delta_z}\right)^2$	$e^{-w^2\sigma_z^2}$
$H_{2,x}$	$\left(\frac{\sin 2u\Delta_x}{2u\Delta_x}\right)^2$	$e^{-4u^2\sigma_x^2}$
$H_{2,y}$	$\left(\frac{\sin 2v\Delta_y}{2v\Delta_y}\right)^2$	$e^{-4v^2\sigma_y^2}$
$H_{2,z}$	$\left(\frac{\sin 2w\Delta_z}{2w\Delta_z}\right)^2$	$e^{-4w^2\sigma_z^2}$
$H_{3,x}$	$\left(\frac{\sin u\Delta_x}{u\Delta_x}\right)^2\left(\frac{\sin 2u\Delta_x}{2u\Delta_x}\right)$	$e^{-3u^2\sigma_x^2}$
$H_{3,y}$	$\left(\frac{\sin v\Delta_y}{v\Delta_y}\right)^2\left(\frac{\sin 2v\Delta_y}{2v\Delta_y}\right)$	$e^{-3v^2\sigma_y^2}$
$H_{3,z}$	$\left(\frac{\sin w\Delta_z}{w\Delta_z}\right)^2\left(\frac{\sin 2w\Delta_z}{2w\Delta_z}\right)$	$e^{-3w^2\sigma_z^2}$
$H_{4,x}$	$\left(\frac{\sin u\Delta_x}{u\Delta_x}\right)^4$	$e^{-2u^2\sigma_x^2}$
$H_{4,y}$	$\left(\frac{\sin v\Delta_y}{v\Delta_y}\right)^4$	$e^{-2v^2\sigma_y^2}$
$H_{4,z}$	$\left(\frac{\sin w\Delta_z}{w\Delta_z}\right)^4$	$e^{-2w^2\sigma_z^2}$

4. Example of EIRP Degradation In Antenna Arrays

To explore the utility of the EIRP degradation, a probabilistic analysis on a simple linear phased array antenna as shown in Figure 1 is performed. Using this example, we investigate how the EIRP degradation behaves as a function of the various parameters.

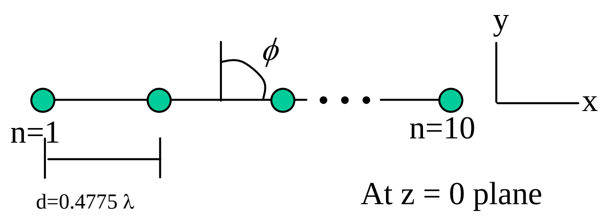

Figure. 1: The Uniformly spaced linear array configuration

Consider a linear array consisting of 10 elements as shown in Figure 1. The array consists of 10 isotropic omni-directional point radiators and is fed by 10 amplifiers. The elements of the linear array are equally spaced and their inter-element spacing along the x-direction is given by 0.4775λ (λ=1m), where λ denotes the wavelength of operation. To simplify the example, we assume that all the elements are located at z = 0 so that the z-positions of all the elements are fixed. Therefore the EIRP degradation of the linear array is caused by random perturbations in the x and y position which can have two types of probability distribution, either uniform or Gaussian. $\overline{H}_z$ is 1 in the Expected value of eq.(21) and $H_{*,z}$ is also 1 in the second moment of the power of eq.(24). When the positions of all the elements are unperturbed, $\overline{H}_x$ and $\overline{H}_y$ equal unity, and also $\overline{P}$ becomes the unperturbed power P_0. As we expect, the variance is identically zero, as given by eq.(23).

The expected value and the standard deviation now is applied to the linear array case to get the normalized EIRP degradation with n = 3 and $[\overline{P} - 3\sigma(P)]/P_0$. Of special interest is the EIRP degradation within the half power beam width between ϕ = 90° and ϕ = 95.33°. Figures 2 and 3 show the worst case degradation with $3\sigma(P)$. Figure 2 represents the case for the Gaussian

perturbation with $\sigma_{x \text{ and } y}$ = 0.0, 0.03, 0.05, and 0.07 [m], and Figure 3 deals with uniform perturbation with $\Delta_{x \text{ and } y}$ = 0.0, 0.03, 0.05, and 0.07 [m]. As expected, the unperturbed case shows a 0 dB value for all the angles. The EIRP degrades with the larger standard deviation of the Gaussian perturbation and the uniform bounds for a uniform perturbation. The EIRP due to the random positions of the antennas is significantly decreased.

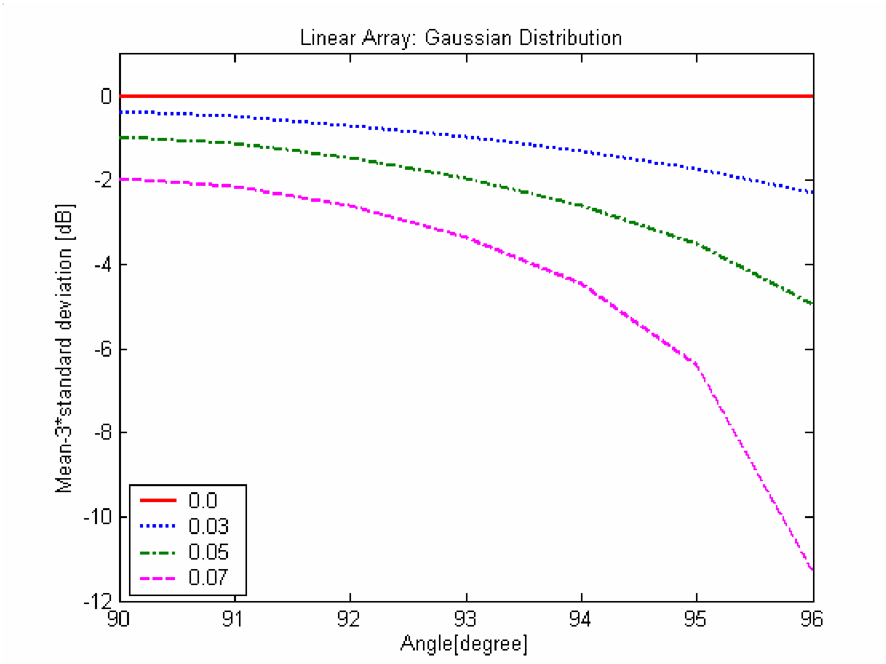

Figure. 2: Normalized EIRP degradation with n = 3 for Gaussian perturbation with standard deviation of $\sigma_{x \text{ and } y}$ = 0.0, 0.03, 0.05, and 0.07 [m]

The normalized EIRP degradation, $[\overline{P} - 3\sigma(P)]/P_0$, represents the worst case for 99.7 percent of all possible cases as mentioned before. This value, however, depends on different values of σ for a Gaussian distribution or has a different Δ for a uniform distribution, as we see from Figures 2 and 3. The question is what is the allowable tolerance for σ and Δ and for the elements to operate appropriately in the antenna system for adaptive signal processing. We focus on the main lobe, especially inside the half power beam width. To choose the appropriate $\sigma_{x \text{ and } y}$ and $\Delta_{x \text{ and } y}$, we select the point that makes the 3dB loss below the optimum for the normalized EIRP degradation graph, at the angle corresponding to the half power beam width. At this –3 dB

point, the antenna performance using conventional beam forming will be significantly decreased. However, the 3dB loss of the normalized EIRP degradation at the angle of the half power beam is the allowable worst case for an antenna system to operate properly compared to the unperturbed case. From these σ and Δ obtained from the 3dB loss point of the normalized EIRP degradation, we investigate how the system behaves if the antenna elements are randomly perturbed by those σ and Δ.

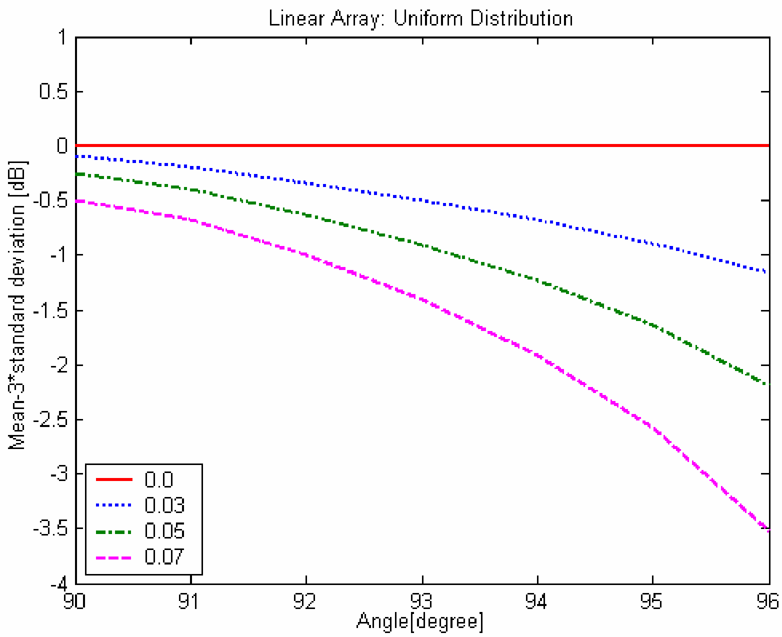

Figure. 3: Normalized EIRP degradation with n = 3 for uniform perturbation with different bounds of $\Delta_{x \text{ and } y}$ = 0.0, 0.03, 0.05, and 0.07 [m].

As illustrated in Figure 4, the −3dB point of the normalized EIRP degradation with n=3 of a uniform linear array occurs at 95.33° with $\sigma_{x \text{ and } y}$ = 0.042 m and $\Delta_{x \text{ and } y}$ = 0.072 m. Figure 4 also illustrates that the relationship between the normalized EIRP degradation with n=3 and $\sigma_{x \text{ and } y}$, and between the normalized EIRP degradation and $\Delta_{x \text{ and } y}$ at a specific angle, 95.33°. The larger the $\sigma_{x \text{ and } y}$ and $\Delta_{x \text{ and } y}$, the lower the normalized EIRP degradation. We apply this value, $\sigma_{x \text{ and } y}$ = 0.042 m and $\Delta_{x \text{ and } y}$ = 0.072 m, and then investigate how the random position errors affect the D^3LS approach for STAP.

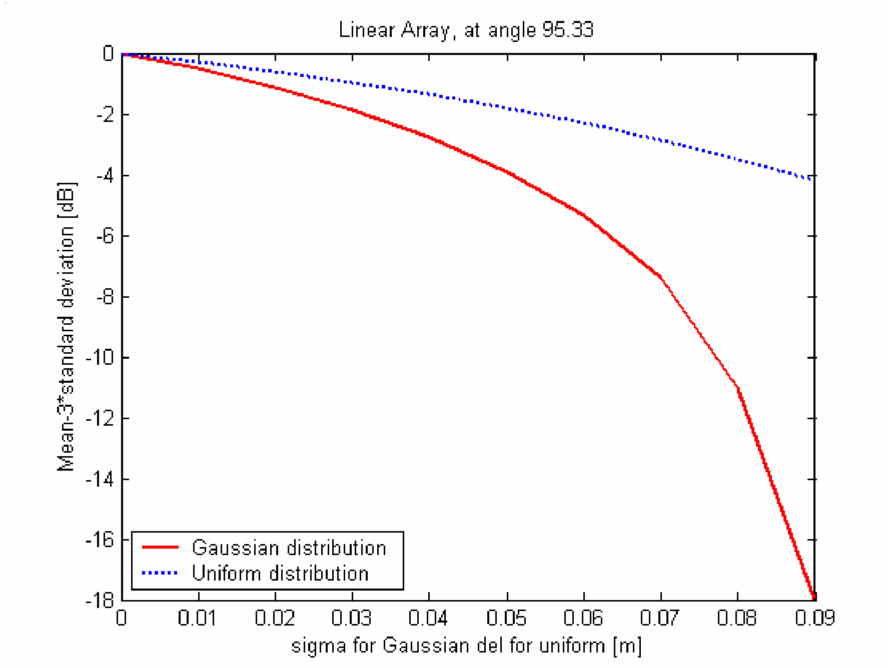

Figure. 4: The relationship between the normalized EIRP degradation with n = 3, and $\sigma_{x \text{ and } y}$ and $\Delta_{x \text{ and } y}$ at the angle, 95.33° for a linear Array.

5. Simulation Results

The received signals modeled in this simulation consist of the SOI, main beam clutter, discrete interferers, jammers and thermal noise. The clutter is modeled as point scatterers placed approximately every 0.1 degrees apart. The amplitude of the clutter points is modeled with a normal distribution about a mean that result in a signal to clutter ratio, SCR, of –12.7 dB. Ten strong point scatterers are modeled in this simulation, based on the angle of arrival (AOA) and Doppler parameters as defined in Table 3. Thermal noise generated in each receive channel is independent from one another. The resulting SNR is approximately 30 dB. The jammer is modeled as a broadband noise signal that arrives from 100° in azimuth, and covers all Doppler frequencies of interest. Summing the power of the interfering sources received by the first channel and comparing it to the power of the SOI, the average input signal to interference plus noise ratio (SINR) is evaluated as –18.6 dB. And random position errors of the antenna element

are $\sigma_{x \text{ and } y}$ = 0.042 m and $\Delta_{x \text{ and } y}$ = 0.072 m. While processing the signal, the antenna elements are randomly moved. In this simulation we consider two situations. One in which the antenna elements at every pulse repletion interval (PRI) sampling instance have different spatial positions from the previous time instance. Another situation is that the antenna random locations are fixed within a coherent processing interval (CPI).

Table 3: Parameters Related to the Simulation.

<table>
<tr><td colspan="2">Wavelength</td><td>1 m</td><td rowspan="3">Signal</td><td>AOA</td><td>60°</td></tr>
<tr><td colspan="2">Pulse Rep. Freq</td><td>4 kHz</td><td>Doppler</td><td>1169 Hz</td></tr>
<tr><td colspan="2">Number of Antennas</td><td>N = 10</td><td>SNR</td><td>30 dB</td></tr>
<tr><td colspan="2">Number of Pulses</td><td>M = 16</td><td rowspan="2">Jammer</td><td>AOA</td><td>100°</td></tr>
<tr><td colspan="2">Half Power Beam width</td><td>10.66°</td><td>Doppler</td><td>Covers all Doppler frequencies of interest</td></tr>
<tr><td rowspan="2">Process-or</td><td>Forward</td><td>$N_a = 7, N_t = 9$</td><td rowspan="4">Discrete interferes</td><td rowspan="2">AOA</td><td rowspan="2">[85° 120° 40° 35° 30° 140° 100° 70° 50° 125°]</td></tr>
<tr><td>Forward-Backward</td><td>$N_a = 8, N_t = 9$</td></tr>
<tr><td rowspan="2">Clutter</td><td>extent</td><td>Main beam</td><td rowspan="2">Doppler</td><td rowspan="2">[400 −800 1700 −1400 325 −1650 950 −1200 −125 1450] Hz</td></tr>
<tr><td>Point scatterers</td><td>0.1° apart in angle</td></tr>
</table>

With N = 10 channels and M = 16 pulses, the performance of the three D^3LS algorithms, namely the Forward, Backward and the Forward and Backward method is evaluated based on the number of adaptive weights and the output SINR. The Forward and the Backward methods utilize 7 spatial (N_a) and 9 temporal (N_t) degrees of freedom (DOF) resulting in a total of 63 DOF, while the Forward-Backward method employs 8 spatial and 9 temporal DOF, for a total of

72 DOF. The spectrum of the input signal is shown in Figure 5. Here the circles indicate the locations of the discrete interferers and the triangles define the location of the main beam clutter and the + mark indicates the location of the SOI.

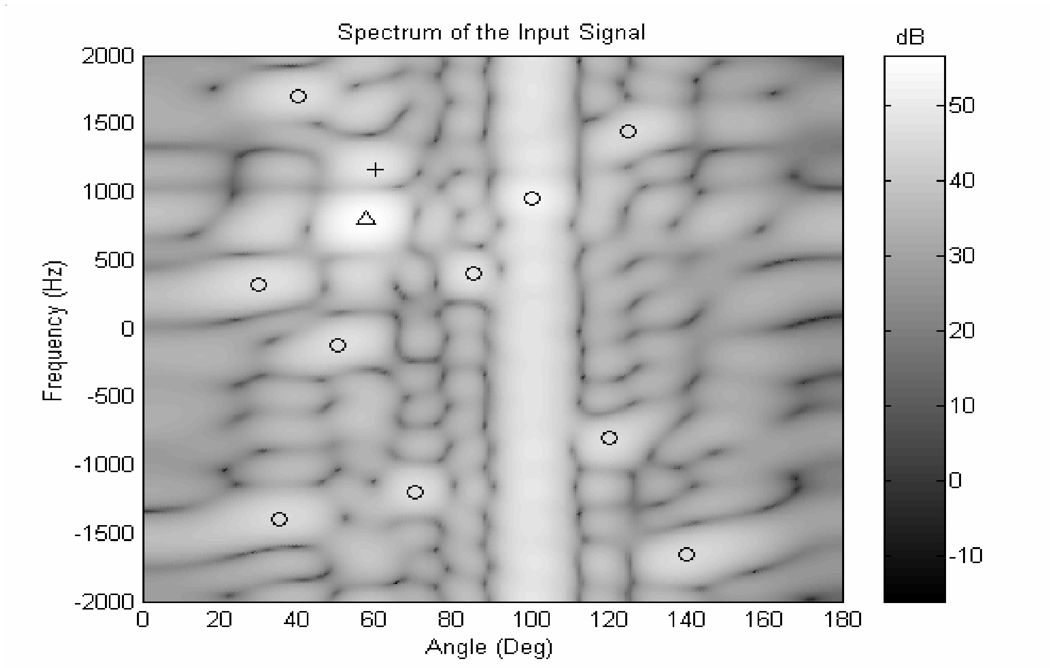

Figure. 5: The spectrum of the Input Signal.

Table 4 shows the output signal-to-interference-plus-noise-ratio (SINR) for the unperturbed case, and perturbed case with a Gaussian profile, and a uniform profile. These values are averaged over 100 runs. The resulting weights for the unperturbed case and for the perturbed case with Gaussian and uniform density functions using the Forward method are shown in Figure 6, 7 and 8, when the antenna elements at every time instance have different spatial positions from the previous time instance. Antenna positions are randomly located with $\sigma_{x \text{ and } y} = 0.042$ m or $\Delta_{x \text{ and } y} = 0.072$ m. The Output SINR of a Gaussian and uniformly perturbed cases are lower than the Output SINR of the unperturbed case. Even though we choose different σ and Δ, we get approximately an output SINR of ±11dB. This shows that we get EIRP degradation which can be obtained analytically. From Figures 7 and 8, the system with random positions generates nulls slightly moved from the angle of arrival (AOA) of discrete interferers as compared to the unperturbed case. The output SINR of the unperturbed case is about 18-19 dB and the output

SINRs for the Gaussian and uniform density distributions, which are about 11 dB when the antenna elements at every time instance have different spatial positions from the previous time instance. This perturbed system still removes the jammer, clutters, discrete interferers and noise. When the random locations of the antenna are fixed in a CPI, one also obtains almost the same output SINR. The value of the output is dependent on the value of the tolerance of the antenna elements.

Table 4: The output signal to interference plus noise ratio.

		Case A (When antenna random locations are changed at every time instance)	Case B (When antenna random locations are fixed in a CPI)
Forward	Unperturbed	18.210 [dB]	
	Gaussian	11.458 [dB]	11.028 [dB]
	Uniform	11.480 [dB]	10.515 [dB]
Backward	Unperturbed	18.210 [dB]	
	Gaussian	11.458 [dB]	11.028 [dB]
	Uniform	11.480 [dB]	10.515 [dB]
Forward-Backward	Unperturbed	19.213 [dB]	
	Gaussian	11.481 [dB]	11.150 [dB]
	Uniform	11.844 [dB]	11.183 [dB]

From these results, as long the antenna element position errors are within the limits set by $\sigma = 0.042$ m for the Gaussian distribution and $\Delta = 0.072$ m for the uniform distribution, the adaptive array has a reasonable performance for STAP. If we want to provide stricter tolerances in the distribution of the antenna elements, i.e., $\sigma < 0.042$ m for the Gaussian distribution and $\Delta < 0.072$ m for the uniform distribution, then one can get higher output SINR which may be close to the output SINR for the unperturbed case. As a result, one can predict how much the system would be degraded by analytically solving the problem using the normalized EIRP degradation.

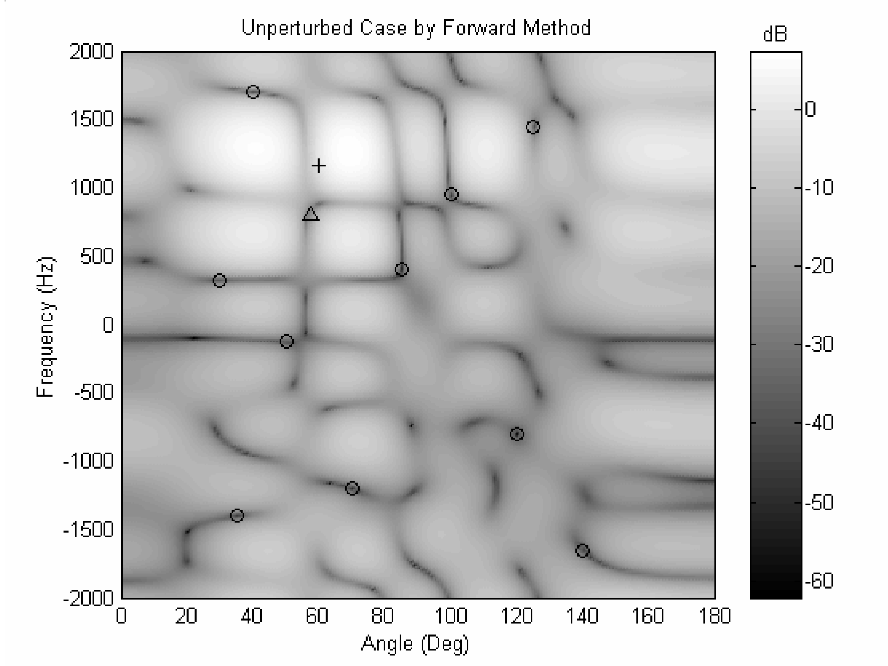

Figure. 6: Weight Spectrum of the Forward Method for the unperturbed case.

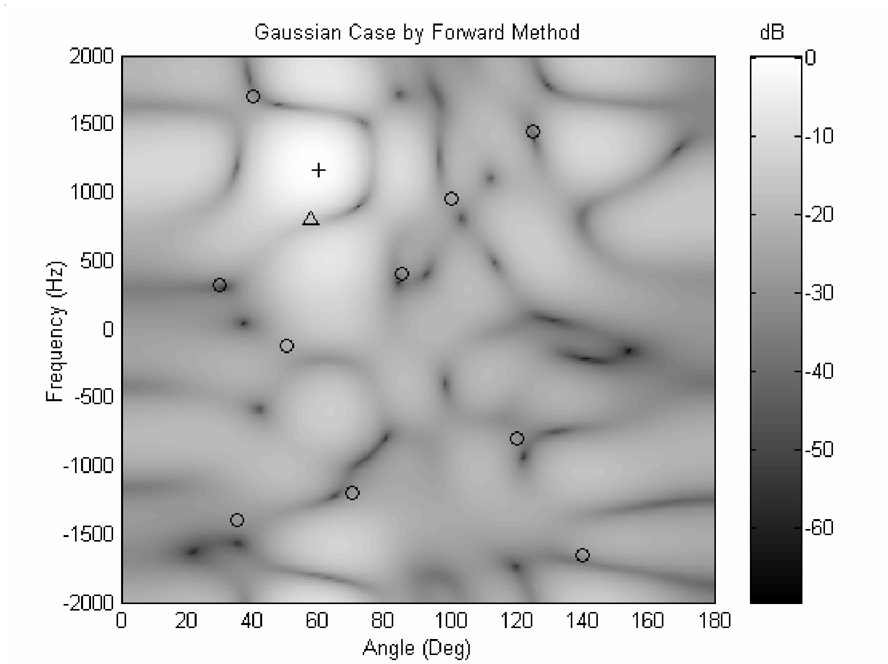

Figure. 7: Weight Spectrum of the Forward Method for the perturbed Gaussian profile with $\sigma_{x \text{ and } y} = 0.042$ m.

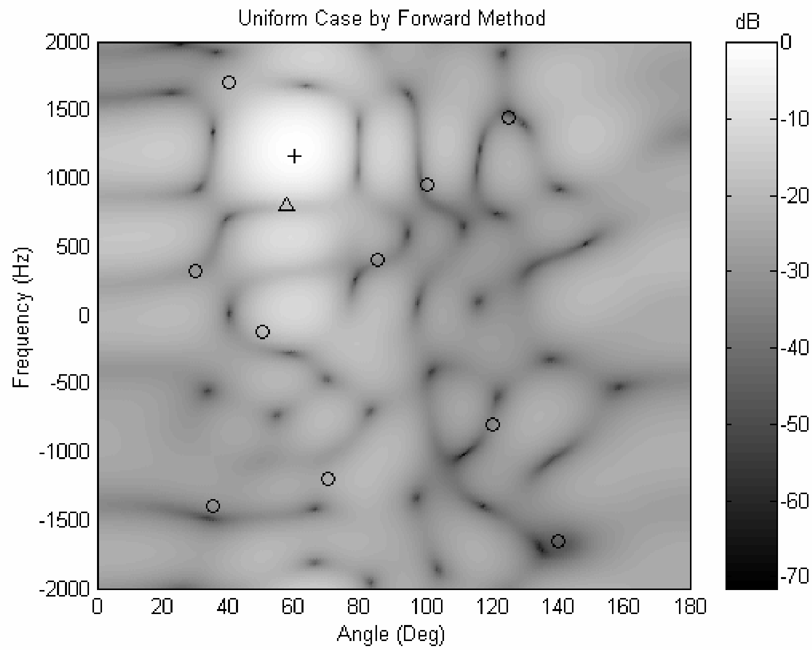

Figure. 8: Weight Spectrum of the Forward Method for the perturbed Uniform profile with $\Delta_{\text{x and y}}$ = 0.072 m.

6. Conclusion

In this report, expressions are derived for the expected value, standard deviation, and the normalized EIRP degradation with n=3 due to the random locations of the array elements. The normalized EIRP degradation represents the worst case for 99.7 percentile of all possible cases. We investigate the effects of random antenna positions on a D^3LS approach for STAP using these EIRP degradations according to the random position of the array elements. Even though σ = 0.042 m for the Gaussian distribution and Δ = 0.072 m for the uniform distribution are given for the antenna elements, we can still get an acceptable output SINR. When the antenna elements at every time instance have different spatial positions from the previous time instance, the output SINR is almost the same as in the case where the antenna elements are located at fixed random locations within a CPI. In this report, the results for the EIRP degradation have been predicted for the Gaussian and for the uniformly perturbed cases. Random antenna position errors degrade the output SINR of a D^3LS Approach for STAP.

7. References

[1] T. K. Sarkar and N. Sangruji, “An Adaptive Nulling System for a Narrowband Signal with a Look Direction Constraint Utilizing the Conjugate Gradient Method”, *IEEE Transactions on Antenna and Propagation*, Vol. 37, pp. 940-944, July 1989.

[2] R. Schneible, “*A Least Square Approach for Radar Array Adaptive Nulling*”, Doctoral Dissertation, Syracuse University, May 1996.

[3] T. K. Sarkar, J. Koh, R. Adve, R. Schneible, M. Wicks, S. Choi and M. Salazar-Palma, “A Pragmatic Approach to Adaptive Antennas”, *IEEE Antennas and Propagation Magazine,* Vol. 42, No. 2, April 2000, pp. 39-55.

[4] T. K. Sarkar, S. Park, J. Koh and R. A. Schneible, “A Deterministic Least Squares Approach to Adaptive Antennas”, *Digital Signal Processing – A Review Journal,* Vol. 6, pp.185-194, 1996.

[5] S. Park,“*Estimation of Space-Time Parameters in Non-homogeneous Environment*”, Doctoral Dissertation, Syracuse University, May 1996.

[6] T. K. Sarkar, H. Wang, S. Park, J. Koh, R. Adve, K. Kim, Y. Zhang, M. C. Wicks and R. D. Brown, “A Determinstic Least Square Approach to Space Time Adaptive Processing (STAP)”, *IEEE Trans. on Antenna and Propagation*, Vol. 49, pp. 91-103, January 2001.

[7] J. T. Carlo, T. K. Sarkar and M. C. Wicks, “A Least Squares Multiple Constraint Direct Data Domain Approach for STAP”, *IEEE Radar Conference Proceedings*, pp. 431-438, 2003.

[8] T. K. Sarkar, M. C. Wicks, M. Salazar-Palma, and R. J. Bonneau, *Smart Antennas*, Wiley-IEEE Press, 2003.

[9] A. I. Zaghloul, “Statistical analysis of EIRP degradation in antenna arrays,” *IEEE Trans. Antennas Propagat.*, Vol. AP-33 pp. 217-221, Feb. 1985.

[10] P. Snoeij and A. R. Vellekoop, “A statistical model for the Error bounds of an active phased array antenna for SAR applications,” *IEEE Trans. Geosci. Remote Sensing*, vol. 30 pp. 736-742 July 1992.

[11] A. Papoulis, *Probability, Random Variables, and Stochastic Processes*, McGraw-Hill, 3rd ed, 1991

[12] S. Hwang and T. K. Sarkar, “Allowable Tolerances in the Position of Antenna Elements in an Array Amenable to Adaptive Processing”, will be published in the *Microwave and Optical Technology Letters*, Nov., 2004.